Energy Science & Engineering

WILEY

ORIGINAL ARTICLE OPEN ACCESS

Performance Comparison of Monocrystalline, Polycrystalline, Low Concentrated, and Bifacial PV Modules in a Particular Geographic Location of South India

Meenatchi Sundaram Palanisamy[1] | Prince Winston David[1] | Palpandian Murugesan[2] | Praveen Kumar Balachandran[3,4] | Pravin Murugesan[5] | Muhammad Ammirrul Atiqi Mohd Zainuri[6] | Mattia Braggio[7] | Vigneselvan Sivasubramaniyam[7]

[1]Department of Electrical and Electronics Engineering, Kamaraj College of Engineering and Technology, Virudhunagar, Tamil Nadu, India | [2]Department of Electrical and Electronics Engineering, AAA College of Engineering and Technology, Sivakasi, Tamil Nadu, India | [3]Departmentof Electrical and Electronics Engineering, Vardhaman College of Engineering, Hyderabad, Telangana, India | [4]Department of Electrical and Electronics Engineering, Chennai Institute of Technology, Chennai, Tamilnadu, India | [5]Departmentof Electrical and Electronics Engineering, National Institute of Technology, Tiruchirapalli, Tamil Nadu, India | [6]Department of Electrical, Electronic and Systems Engineering, Faculty Engineering and Built Environment, Universiti Kebangsaan Malaysia, Bangi, Selangor, Malaysia | [7]Department of Mechanical, Chemical and Material Engineering, University of Cagliari, Cagliari, Italy

Correspondence: Praveen Kumar Balachandran (praveen@ukm.edu.my) | Prince Winston David (dpwtce@gmail.com)

Received: 22 July 2025 | **Revised:** 25 November 2025 | **Accepted:** 5 February 2026

Funding: This research work is supported by Universiti Kebangsaan Malaysia research grants, Grant/Award Numbers: DPK-2023-015, KK-2023-009

Keywords: module efficiency | performance ratio | power loss | PV module | solar irradiation | temperature

ABSTRACT

This study presents a performance comparison of four commercially available photovoltaic (PV) modules: polycrystalline PV module (PPVM), monocrystalline PV module (MPVM), low-concentrated PV module (LPVM), and bifacial PV module (BPVM). The experiment was conducted to investigate the effects of irradiation and temperature on PV modules in the same geographic location. The study results showed that the module's performance exhibits strong dependence on irradiation and temperature. The module's operating temperature has a significant impact on the efficiency. The performance ratio and module efficiency show an increasing trend with increasing irradiation. The P.U. power of BPVM was 4% more than that of PPVM and LPVM and 11% more than MPVM. At both low and high irradiation levels, the BPVM module showed better efficiency. At the highest irradiation, the module efficiency of BPVM was 51.2% higher than that of PPVM and 64% higher than that of LPVM and MPVM. The performance ratio of BPVM is 3% higher than PPVM, 7% higher than LPVM, and 11% higher than MPVM. Compared with PPVM, MPVM, and LPVM, the BPVM has improved P.U. power, module efficiency (22.79%), and performance ratio by 64%, 60%, and 70%, respectively. The experimental results show that selecting an optimal PV module for a given location enhances its efficiency.

1 | Introduction

The Indian national power grid is well-suited to integrating renewable energy sources due to the country's political, economic, and energy situation. Among the existing renewable energy sources, solar photovoltaic (PV) is found to be abundant and pollution-free [1]. The PV system has experienced rapid growth and has been implemented across different regional conditions due to its scalability and adaptability. The size of PV ranges from stand-alone systems to megawatt-scale centralized power plants. The hot, sandy and cold region with high

[Correction added on 1 April 2026, after first online publication: The authors "Mattia Braggio" and "Vigneselvan Sivasubramaniyam" have been added to the author byline.]

altitudes are suitable for the installation of PV system. Thus, the requirement for PV to operate across diverse regions has paved the way for the development of various technologies. Innovations in PV technology have enabled the manufacture of PV modules with lightweight, custom shapes, and transparency [2]. Replacing the aluminum-covered back surface with a passivated emitter rear contact has increased the PV cell's efficiency from 16% to 25%. The improvement in efficiency, with falling prices, has led to the expansion of new materials and technologies [3].

When the PV cells are exposed to solar irradiation, they absorb photons, and electricity begins to flow. The performance of PV modules under incident solar irradiance is influenced by factors such as operating temperature, spatial arrangement, dust, dirt, partial shading, mismatch loss, wiring loss, faults, and inverter loss [4]. The manufacturer's PV module specification in the datasheet, under standard test conditions (STC), does not provide the necessary information on performance at a specific location. For this, International Electrotechnical Commission 61853-1:2011 provides parameters such as high temperature (1000 W/m^2 and 75°C) and low temperature (500 W/m^2 and 15°C). However, this information is not provided by the manufacturer. To identify which PV technologies are most appropriate for the local area, it is crucial to test PV modules in a real-time environment [5]. Module efficiency depends on the design, technology, components, and operating environment. Based on these specifications, limitations, and advancements, four generations of PV cells were developed.

The common material used for developing PV modules is crystalline silicon (c-Si) [6]. Innovation in materials and technology has paved the way for the development of various PV technologies, such as thin-film PV module (TPVM), low-concentrated PV module (LPVM), flexible PV modules, double-glass PV modules, bifacial PV module (BPVM), smart PV modules, and so forth. The significant improvements in technology across each module generation include reduced costs, enhanced durability, and improved module efficiency. However, there are advantages and disadvantages to each PV technology, which become clear when testing is conducted in a real-time environment [7].

The global PV market is dominated by the c-Si PV modules of two different types, namely monocrystalline PV module (MPVM) and polycrystalline PV module (PPVM). The mono c-Si PV cells are manufactured from the c-Si ingot, which is cut into a wafer less than 0.3 mm thick. The mono c-Si PV cell fabricated on this wafer is capable of generating a voltage and current of 0.55 V and 35 mA under fully illuminated conditions. These mono c-Si PV cells are grouped into a module. The main reason behind the expansion of MPVMs is their low cost. The drawbacks of mono c-Si PV cells include high cost and a decrease in efficiency at 25°C. In addition, mono c-Si PV cells are prone to metal contamination, leading to the formation of PPVM.

The PPVM is produced from metallurgical-grade silicon. The poly c-Si PV cells are fabricated from a molten vat rather than a single ingot and are grouped to form modules. Compared to mono c-Si PV cells, poly c-Si PV cells have different crystal structures, which minimize light reflection and, consequently, improve their efficiency [8]. The c-Si cell experiences higher temperature-related power loss (PL) in winter than in summer [9, 10]. The c-Si module suffers power degradation of 0.5%–1.5% during the initial hour of exposure and becomes less vulnerable to fluctuations in the solar spectrum by ~1%–2% [11, 12]. At higher temperatures, c-Si PV modules degrade in power and module efficiency. As the bandgap decreases, the open-circuit voltage (V_{oc}) decreases linearly. Furthermore, this may decrease the power conversion and maximum power. Meanwhile, rising temperature increases the short-circuit current (I_{sc}), but this increase cannot compensate for the performance degradation caused by the other parameters [13, 14].

The main intention of the PV industry is to develop a cost-effective TPVM as an alternative to the c-Si PV module. The TPVM is formed from a semiconductor material sealed by lamination and positioned between two sheets of glass. An anti-reflection coating is applied to the surface to reduce light reflection. A module consists of several thin-film cells, and they are wired together. TPVM consists of several thin, absorbing layers with thicknesses ranging from a few nanometers to tens of micrometers; hence, its manufacturing cost is low. TPVM suffers from lower power density and very low durability compared to c-Si. TPVM has been used for consumer products, where c-Si is found to be unsuitable [15].

The TPVMs are classified as Amorphous Silicon (a-Si), cadmium telluride (CdTe), copper indium gallium selenide (CIGS), and gallium arsenide (GaAs). The direct band gap material of a-Si allows a fraction of sunlight within a thin layer of a few micrometers. Compared to c-Si, the advantage of a-Si is that it requires a very small quantity of active material. At low solar radiation levels and diffuse radiation, the a-Si PV has significant module efficiency. Compared with the c-Si module, the output power is less affected by the cell temperature. In the higher power range, glass–glass-encapsulated a-Si PV modules are considered for the building-integrated applications. The production cost for a-Si is dominated by the non-active material. Therefore, the advantage of a-Si is that the module costs are not dependent on silicon and have a shorter payback period.

a-Si has a short diffusion length and is vulnerable to high solar irradiation and low charge mobility [15]. Despite development over the years, CdTe has not been able to hold its market share. In the last few years, it has obtained significant growth and dominates the PV market compared to the c-Si PV module. The advantage of the CdTe PV module is its low cost and high module efficiency. The main drawback of TPVM is the toxicity of the Cd material. Hence, proper recycling is essential to overcome these drawbacks [16, 17]. The CIGS module is produced from a direct-bandgap material with a band gap of 1.0 to 1.7 eV. It has obtained a record module efficiency of 0.5%. By changing the bandgap of germanium and silicon, the module efficiency of the CIGS module can be improved [17]. Furthermore, the module efficiency can be improved by incorporating an alkaline material, such as sodium. Sodium causes defects at grain boundaries, which are the main factor limiting its module efficiency [17, 18].

The direct bandgap of 1.43 eV in GaAs, produced by deposition methods, enables a module efficiency of up to 25.1 ± 0.8%. Several advanced technologies available on the market include quantum dot solar cells, organic solar cells, and copper-zinc-tin sulfide solar cells [19]. Among the TPVM technologies, a-Si has complex electrical characteristics. Compared to multi-crystalline silicon and polycrystalline silicon technologies, it has a lower temperature-related PL coefficient of −0.21 to −0.30%/K, and a nominal power tolerance is ±12% [20, 21]. Therefore, it exhibits higher performance during the summertime and is suitable for operation in hot or tropical climates [22, 23].

TPVM generates more power on cloudy days due to diffuse irradiation and is less dependent on the angle of inclination. Compared to c-Si technology, it is less sensitive to variation in the solar spectrum. Like crystalline technology, the efficiency of copper indium diselenide (CIS) and CdTe decreases during the summer and increases during the winter months [23]. During the initial hours of exposure to solar irradiance, the TPVM undergoes performance degradation. The a-Si technologies suffer degradation at a nominal power of 0.8% until their stabilization [24]. However, in CIS technology, during the first hour of exposure to sunlight, its efficiency increases by 7%–15%. However, the efficiency of CdTe increases by 6%–8% or decreases by 7%–15% based on the design and manufacturing process [25–27]. The performance of TPVM relies on the temperature, light intensity, wind, and dust accumulation. Due to its lower temperature coefficient, the TPVM is less sensitive than c-Si PV modules. Therefore, it delivers higher power at higher temperatures [27].

Concentrated PV (CPV) cells generate electricity by concentrating sunlight using mirrors and optics. The optics may be Fresnel lenses and Cassegrain primary reflectors to focus the sunlight throughout the day [28]. The CPV system is mainly used to generate electricity at high levels of direct normal irradiance over 2000 $kWh/(m^2a)$. Therefore, it is normally preferred for space applications [29, 30]. CPVs can be classified as high CPV (HCPV) and LPVM based on the levels of concentrators.

The III-V semiconductor group of HCPVs built with double-axis sun trackers has a higher module efficiency of up to 40%. However, the cost of the CPVs has reduced over the years. LPVMs are composed of c-Si and are built with single-axis or double-axis trackers to concentrate sunlight to below 100 suns. LPVMs are produced on some instances with c-Si cells, which opens up the market. The design of the compound parabolic concentrator results in a very high reflectance of incident light to the absorber. Because it can focus sunlight over a wide range, its module efficiency is higher. Because of the concave structure, the system does not require tracking, thereby lowering costs [29, 30].

The existing PV technologies are mono-facial PV modules capable of generating electricity from solar irradiation. The mono-facial PV module is installed in an open rack and generates power only from direct and diffuse solar irradiation. The mono-facial PV module cannot utilize the reflected component of solar irradiation [31]. However, the BPVM can generate electricity on both the front and rear sides.

The BPVM can generate electricity from the direct, diffuse, and reflected components of solar irradiation, especially at high albedo and high latitudes [32]. Power generation from the rear side varied with different reflective conditions [33]. The capability of the BPVM to extract more power is termed bifacial gain. The power gain of BPVM was 25% higher than that of MPVM under the optimized installation conditions [34]. The fabrication of BPVM is only 3% higher than MPVM, resulting in a small increase in module cost and a higher energy yield [35, 36]. The parameters, such as installation conditions, irradiance, and mismatch effects, for BPVM are to be assessed and compared with those for MPVM. Among these parameters, mismatch is a dominant factor that affects the long-term reliability of BPVM [37, 38]. Table 1 presents the performance comparison of various PV module technologies.

From the literature review, it is evident that each PV module technology has its own merits and demerits when exposed to outdoor conditions. Hence, it is the need of the hour to determine the optimal module for a particular geographical location. Hence, a keen understanding of PV modules is essential for extracting superior performance in outdoor environments. This study aims to compare the performance of irradiation and temperature across different commercially available PV modules, including PPVM, MPVM, LPVM, and BPVM. Here, the TPVM is not considered in the analysis due to its toxic nature. This study has considered the LPVM because researchers have not focused on it due to the higher area requirement for power generation compared to other module technologies. Therefore, it is necessary to test the different modules in an outdoor environment to evaluate power P.U. area, P.U. power, module efficiency, PL, and performance ratio (PR).

1.1 | Novelty of Proposed Study

- To conduct the performance comparison of irradiation and temperature on different commercially available PV modules like PPVM, MPVM, LPVM, and BPVM.
- This study has considered the LPVM because researchers have not focused on it due to the higher area requirement for power generation compared to other module technologies.
- For validation, the different modules are tested under an outdoor environment in terms of P.U. area, P.U. power, module efficiency, PL, and PR.

The organization of this study is as follows: Section 2 demonstrates the experimental setup and performance parameters, Section 3 elaborates on the results and discussion, and Section 4 concludes the study.

2 | Experimental Setup

The four commercially available PV modules (PPVM, MPVM, LPVM, and BPVM) used in this study are installed on the rooftop of Kamaraj College of Engineering & Technology, K. Vellakulam, at the latitude of 9.6728° N and longitude of 77.9659° E, as shown in Figure 1. All the PV modules are mounted on a fixed installation at a tilt angle of 9.67° facing south.

Table 2 describes the electrical characteristics of the PV modules. The PV modules were well exposed to solar radiation, with minimal shading due to the sun's movement. The experimental setup is shown in Figure 2.

TABLE 1 | Survey on performance comparison of various PV modules.

References	Crystalline PV module		TPVM								
	m-S$_i$	p-S$_i$	Multicrystalline	a-S$_i$	C$_d$T$_e$	CIS	HIT	LPVM	BPVM	Region	Remarks
[39]	—	√	—	√	—	—	—	—	—	Kobe, Japan	• a-Si performed better • PR value of p-Si decreased with an increase in temperature increased • a-Si and p-Si solar cells have the response on V_{oc} and I_{sc} for the influence of irradiation and temperature
[40]	√	√	—	√	—	—	—	—	—	Desert, Helwan	• p-Si performed better in the infrared region
[41]	√	√	—		—		√	—	—	Japan	• Because of its low temperature dependency, the heterojunction with intrinsic thin layer (HIT) technology is ideal for this region
[42]	√	√	—	√	—	√	—	—	—	Western Australia	• a-Si produced 8% to 15%
[43]		√	√	√	—		—	—	—	Japan	• p-Si performed better when compared to a-Si under the spectral irradiation distribution
[44]	√	√	√	√	—	√	—	—	—	Malaysia	• At high temperature, m-Si and p-Si delivered better results • Furthermore, a-Si is preferred in cloudy weather
[45]	√		√	√	—	—	—	—	—	Norway	• m-Si delivered better results
[46]	√	√	—	√	—	—	—	—	—	South Africa	• m-Si, p-Si, and a-Si exhibited similar results
[47]	—	√	—	√	—	—	√	—	—	India	• Compared to p-Si, the HIT and a-Si performed better
[48]	√	—	—	√	—		√	—	—	Italy	• a-Si modules have delivered better results
[49]	—	—	—	—	—	√	—	—	—	Kuwait	• The average PV performance ratio was no less than 0.7
[50]	√	√	—	√	—	—	—	—	—	Sudano-Sahelian climate	• a-Si has delivered a PR of 92%
[51]	√	√	√	√	√	√	—	—	—	Brazil	• c-Si modules suffered due to high relative humidity and temperature
[52]	√							√		London, England	• LPVM has performed better compared to m-Si in terms of output P.U. area • LPVM found to be a viable option for the study area
[53]		√							√	Tamil Nadu, India	• On the front side, the BPVM delivered 26% more power and 16% on the rear side compared to the PPVM • BPVM delivered 15% more power on both sides compared to PPVM

FIGURE 1 | Satellite view of the experimental location.

TABLE 2 | Specification of the examined PV modules.

Specifications	PPVM	MPVM	LPVM	BPVM
Maximum power P_{max} (W)	250	250	265	395
Open circuit voltage V_{oc} (V)	37.23	37.23	41.2	46.8
Maximum voltage V_{max} (V)	29.7	29.7	35.5	38.3
Short circuit current I_{SC} (A)	8.95	8.95	9.24	11.8
Maximum current I_{max} (A)	8.42	8.42	7.5	10.3
Temperature coefficient of P_{max} (%/°C)	−0.30%	−0.40%	−0.48%	−0.40%
Temperature coefficient of V_{oc} (%/°C)	−0.27%	−0.31%	−0.34%	−0.31%
Temperature coefficient of I_{sc} (%/°C)	0.06%	0.064%	0.065%	0.065%
Efficiency (%)	14.7	15.5	16.8	22.5
Module area (m^2)	1.69	1.61	1.58	1.75
Color	Blue	Black	Black	Black
Tilt angle (degrees)	9.6	9.6	9.6	9.6
Fill factor	75	75	69.7	71.5

The four commercially available PV modules (PPVM, MPVM, LPVM, and BPVM) are assessed in this study. The specifications of the PV modules were presented in Table 2. The PV modules were installed in a location well exposed to solar radiation, with minimal shading. An electrical load is connected to the PV modules to deliver maximum power via the Solar PCU kit's maximum-power-point-tracking. The electrical variables of the PV module, such as the voltage at maximum power (V_{max}), the current at maximum power (I_{max}), and the maximum power (P_{max}), were measured every hour from 09:00 a.m. to 05:30 p.m. using the measuring instruments. The maximum power point tracking Solar PCU kit (Smarten Make, Prime + 12 to 24 V/30 A Model) is used to deliver the maximum power. At any particular instant, the solar PV module's maximum voltage, current, and power are measured through this maximum power point tracking kit.

The Solar Power Meter (Model: SPM-1116SD) measures instantaneous solar irradiance. To measure the module's operating temperature, the FLIR-E4 thermal imaging camera is used (IR resolution of 4800 pixels). Since the PV module power ratings vary, they are converted to P.U. values for analysis. The performance of the module is analyzed in terms of performance parameters using the subsequent equations.

FIGURE 2 | Experimental setup of PPVM, MPVM, LPVM, and BPVM.

2.1 | Power P.U. Area

The power P.U. area is defined as the ratio of the power generated to the area of the PV module [54].

$$\text{Power per unit area} = \frac{\text{Output power (W)}}{\text{Area of the PV module } (\text{m}^2)}. \quad (1)$$

2.2 | P.U. Power

The P.U. power is defined as the ratio of the measured output power to the maximum power at STC [54].

$$\text{P.U. power} = \frac{100 \times \text{Measured output power (W)}}{\text{Maximum power at STC (W)}}. \quad (2)$$

2.3 | Module Efficiency

The module efficiency is defined as the ratio of the incident irradiation that falls on the module surface to the usable electricity [54].

$$\text{Module efficiency} = \left(\frac{\text{Measured output power} \quad (\text{W})}{(\text{Incident irradiation } (\text{W/m}^2) \times \text{Area of the module } (\text{m}^2))} \right) \times 100. \quad (3)$$

2.4 | PR

The PR is defined as the ratio of the module's performance under outdoor conditions to its performance under STC [54].

$$\text{PR} = \frac{(\text{Measured output power(W)} / (\text{Maximum power at STC(W)})}{(\text{Incident irradiation} (\text{W/m}^2)/1000)}. \quad (4)$$

3 | Results and Discussion

In this study, a comprehensive analysis of the performance of various PV modules is conducted. In particular, the investigation summarizes the impact of incident irradiance and temperature on the PV module performance. Tables 3–5 represent the results of the performance parameters.

3.1 | Solar Irradiation

On December 11, 2021, experimentation was conducted on different PV modules between 09.00 a.m. and 05.30 p.m., and the results were recorded for further analysis. During the experimentation, the incident irradiation is varied between 110 and 940 W/m^2 as depicted in Figure 3. It is observed that a linear relationship between output power and incident irradiance. At 05.30 p.m., the lowest irradiation of 110 W/m^2 is recorded.

TABLE 3 | Experimental results for PPVM.

Time	Irradiation (W/m^2)	Temperature (°C)	V_m (V)	I_m (A)	P_m (W)	P.U. V_{max}	P.U. I_{max}	P.U. P_{mac}	P.U. area P_m	% PL	% η	PR
9.00	350	37.3	28.7	2.9	85	0.966	0.350	0.338	50	66	14.3	0.966
10.00	450	41.2	28.9	3.8	110	0.973	0.450	0.438	65	56	14.4	0.973
11.00	650	47.7	29.2	5.5	160	0.983	0.650	0.639	95	36	14.55	0.983
12.00	890	49.5	29.5	7.5	221	0.993	0.890	0.884	131	12	14.7	0.993
1.00	940	55.6	29.7	7.9	235	1.000	0.940	0.940	139	6	14.8	0.1000
2.00	860	53.3	29.6	7.2	214	0.997	0.860	0.857	127	14	14.75	0.996
2.30	740	50.7	29.5	6.2	184	0.993	0.740	0.735	109	26	14.7	0.993
3.00	580	48.4	29.3	4.9	143	0.987	0.580	0.572	85	43	14.6	0.986
3.30	470	46.7	29.1	4.0	115	0.980	0.470	0.461	68	54	14.5	0.980
4.00	380	41.1	28.8	3.2	92	0.970	0.380	0.369	55	63	14.35	0.970
4.30	290	38.2	28.6	2.4	70	0.963	0.290	0.279	41	72	14.25	0.963
5.00	150	36.3	28.4	1.3	36	0.956	0.150	0.143	21	86	14.15	0.956
5.30	110	36.1	28.2	0.9	26	0.949	0.110	0.104	15	90	14.05	0.949

TABLE 4 | Experimental results for MPVM.

Time	Irradiation (W/m^2)	Temperature (°C)	V_m (V)	I_m (A)	P_m (W)	P.U. V_{max}	P.U. I_{max}	P.U. P_{max}	P.U. area P_m	% PL	% η	PR
9.00	350	37.1	24.8	3.1	77	0.835	0.370	0.309	48	69	13.69	0.881
10.00	450	41.1	25.1	4.0	100	0.845	0.476	0.402	62	60	13.86	0.892
11.00	650	47.5	25.2	5.8	146	0.848	0.688	0.582	90	42	13.91	0.896
12.00	890	49.4	25.3	7.9	200	0.852	0.942	0.801	124	20	13.97	0.899
1.00	940	55.3	25.4	8.4	212	0.855	0.995	0.849	132	15	14.03	0.903
2.00	860	53.2	25.4	7.6	194	0.855	0.910	0.777	121	22	14.03	0.903
2.30	740	50.6	25.3	6.6	166	0.852	0.783	0.666	103	33	13.97	0.899
3.00	580	48.2	25.3	5.2	130	0.852	0.614	0.522	81	48	13.97	0.899
3.30	470	46.6	25.2	4.2	105	0.848	0.497	0.421	65	58	13.91	0.896
4.00	380	40.9	25.1	3.4	85	0.845	0.402	0.339	53	66	13.86	0.892
4.30	290	37.9	24.9	2.6	64	0.838	0.307	0.257	40	74	13.75	0.885
5.00	150	36.2	24.8	1.3	33	0.835	0.159	0.132	21	87	13.69	0.881
5.30	110	36.1	24.7	1.0	24	0.832	0.116	0.097	15	90	13.64	0.878

The BPVM has obtained P.U. power of 0.108 (Figure 4), followed by the PPVM, LPVM, and MPVM of 0.104, 0.104, and 0.097, respectively. At higher solar irradiance above 450 W/m^2, the BPVM obtained an average P.U. power of 0.70, followed by the PPVM, LPVM, and MPVM at 0.69, 0.64, and 0.62, respectively. At 01.00 p.m., maximum irradiation of 940 W/m^2 is recorded. The BPVM has obtained a P.U. output power of 0.960, followed by the PPVM, LPVM, and MPVM at 0.940, 0.854, and 0.849, respectively. Overall, BPVM had the highest average P.U. power of 0.960, followed by PPVM, LPVM, and MPVM at 0.940, 0.854, and 0.849, respectively. Additionally, BPVM has shown improved performance across all irradiance levels due to its power-generating capacity from the direct, diffuse, and reflected components of solar irradiation.

3.2 | Temperature Analysis

The PV module operating temperature depends on incident irradiance and ambient temperature. The PV module operates at a higher temperature than the ambient temperature due to heat generated during energy conversion. The module's temperature increases with increasing incident irradiation. The operating temperature of all the PV modules measured from 09.00 a.m. to 05.30 p.m. is depicted in Figure 5.

At 01.00 p.m., the maximum solar irradiance of 940 W/m^2 is observed, and all the PV modules reach their maximum temperature. The MPVM operates at a lesser temperature of 55.3°C, followed by the PPVM, BPVM, and LPVM at 55.6°C, 58.6°C, and 60.1°C, respectively. The LPVM operates at a higher

TABLE 5 | Experimental results for LPVM.

Time	Irradiation (W/m^2)	Temperature (°C)	V_m (V)	I_m (A)	P_m (W)	P.U. V_{max}	P.U. I_{max}	P.U. P_{max}	P.U. area P_m	% PL	% η	PR
9.00	350	40.1	33.3	2.7	89	0.938	0.357	0.336	56	66	16.1	0.959
10.00	450	47.1	32.8	3.4	113	0.924	0.458	0.426	71	57	15.86	0.944
11.00	650	53	32.7	5.0	162	0.921	0.662	0.613	103	39	15.81	0.941
12.00	890	55	32.1	6.8	218	0.904	0.907	0.824	138	18	15.52	0.924
1.00	940	60.1	31.5	7.2	226	0.887	0.958	0.854	143	15	15.23	0.907
2.00	860	59.2	31.8	6.6	209	0.896	0.876	0.788	132	21	15.38	0.915
2.30	740	56.7	32.2	5.7	182	0.907	0.754	0.687	115	31	15.57	0.927
3.00	580	53.8	32.4	4.4	144	0.913	0.591	0.542	91	46	15.67	0.933
3.30	470	52.6	32.5	3.6	117	0.915	0.479	0.440	74	56	15.72	0.936
4.00	380	47.1	32.8	2.9	95	0.924	0.387	0.359	60	64	15.86	0.944
4.30	290	43.5	33.1	2.2	73	0.932	0.295	0.277	46	72	16.01	0.953
5.00	150	40.6	32.9	1.1	38	0.927	0.153	0.142	24	86	15.91	0.947
5.30	110	39.1	32.7	0.8	27	0.921	0.112	0.104	17	90	15.81	0.941

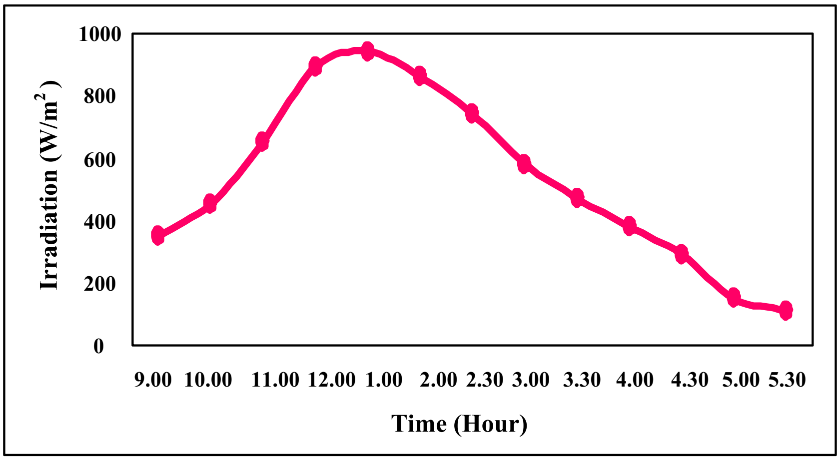

FIGURE 3 | Variation of incident solar irradiation on the PV modules.

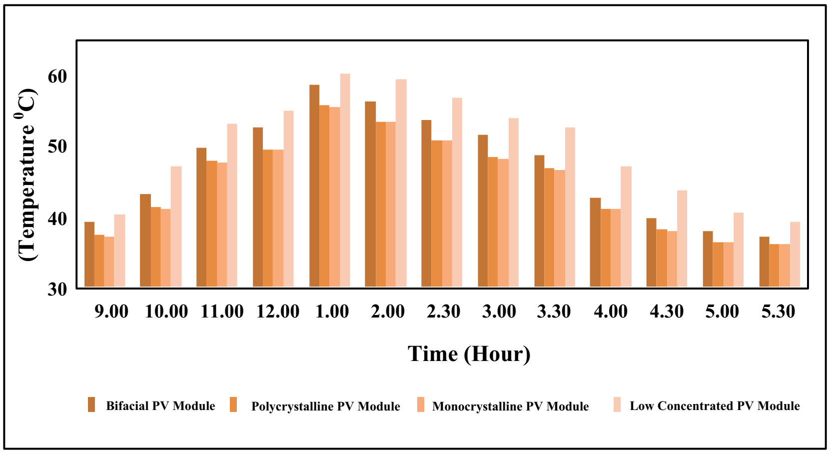

FIGURE 4 | Per unit power of PV module technologies.

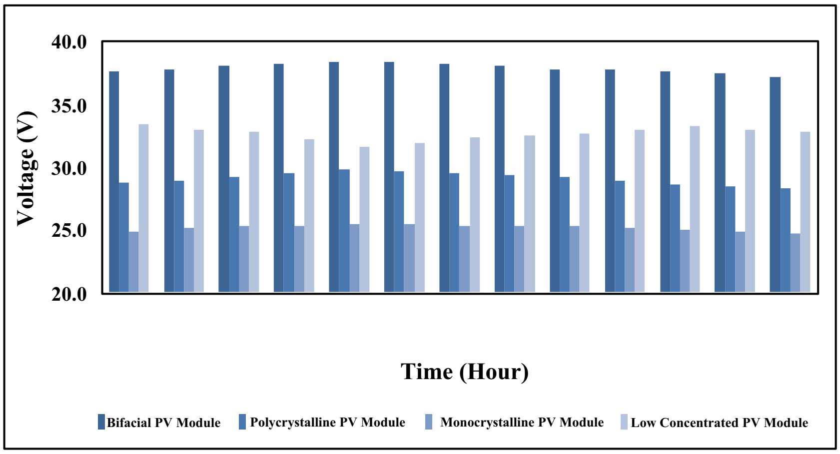

FIGURE 5 | Variation of temperature during experimentation on the PV modules.

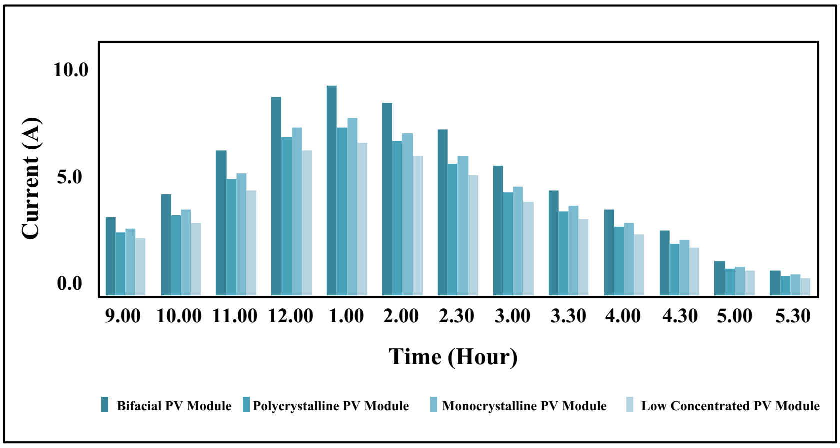

FIGURE 6 | Variation of voltage during experimentation on the PV modules.

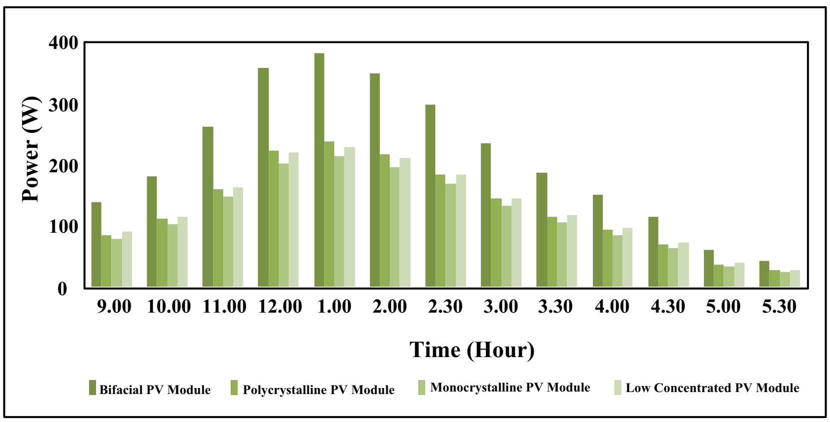

FIGURE 7 | Variation of current during experimentation on the PV modules.

temperature due to internal reflections within the glass concave structure. Figure 6 illustrates the variation of V_{oc} for the increase in temperature of the module. Here, the V_{oc} decreases slightly with increasing temperature. Figure 7 shows the significant increase in I_{sc} with respect increase in temperature. The experimental results show that higher temperature improves the performance of all PV modules.

The peak power is recorded at 55.3°C, 55.6°C, 58.6°C, and 60.1°C for MPVM, PPVM, BPVM, and LPVM, respectively. The reduction in the maximum power is based on the temperature coefficient. The higher temperature coefficient slightly decreases the V_{oc} and increases the I_{sc}, thereby reducing the output power of the PV module, as shown in Figure 8. After 03.00 p.m., the module temperature decreases below the ambient temperature, resulting in an increase in the PV module's output power. The MPVM has the lowest average temperature at 44.62°C, followed by the PPVM, BPVM, and LPVM at 44.77°C, 46.96°C, and 49.83°C, respectively.

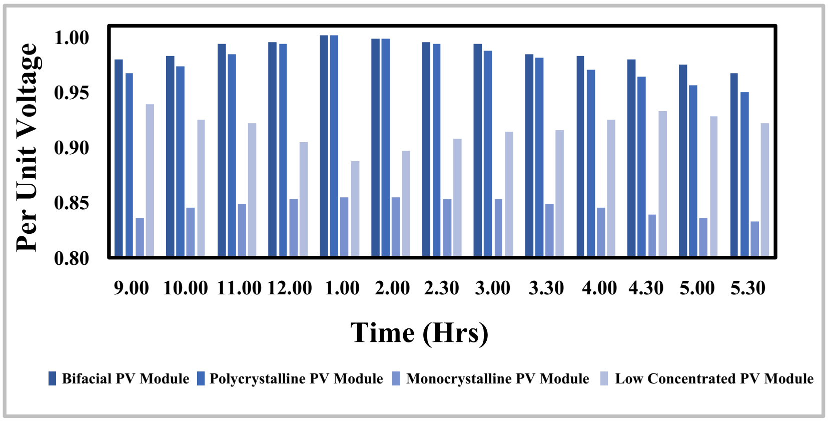

FIGURE 8 | Output power of all the PV modules.

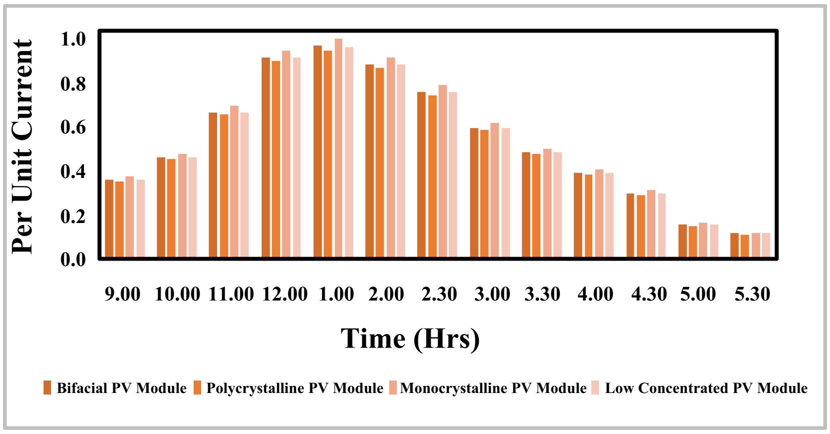

FIGURE 9 | Per unit voltage of PV module technologies.

3.3 | Percentage PL

Figure 9 depicts the variant of the P.U. voltage of all the PV modules. The P.U. voltage BPVM and PPVM are almost similar in most irradiation conditions. The LPVM has obtained a P.U. voltage below BPVM and PPVM, and a higher P.U. voltage than the MPVM. The MPVM has the lowest P.U. voltage among the modules due to its high PL. Figure 10 depicts the variation in the P.U. maximum current across all PV modules, and this P.U. current increases with increasing temperature. The MPVM has delivered higher P.U. current across all irradiation conditions, followed by the BPVM and LPVM, which delivered similar current. The PPVM has obtained the lowest P.U. current among the modules.

Figure 4 depicts the P.U. power of all the PV modules, which depends on the P.U. voltage and current. The reduction in P.U. voltage depends on the PL, significantly reducing the P.U. power. Figure 11 depicts the percentage PL of all the PV modules. At an irradiance of 110 W/m^2, the PL produced by the modules is almost identical. For irradiation between 110 and 540 W/m^2, the PL of all modules is nearly identical. Within the irradiation range of 650–740 W/m^2, PL varies among modules.

For the BPVM and PPVM, the PL decreases with increasing irradiation, and the PLs of both modules are very similar. For the MPVM, PL decreases with increasing irradiation, and the decrease is less than for the MPVM and PPVM. The MPVM has the highest PL among the modules considered for the study. Under high irradiation conditions, the BPVM produced the lowest PL of 4%, followed by the PPVM, LPVM, and MPVM, with PLs of 6%, 15%, and 15%, respectively. The BPVM has delivered superior performance, with an average PL of 47% compared to PPVM, LPVM, and MPVM, by 48%, 51%, and 53%, respectively.

3.4 | Module Efficiency

At irradiance between 740 and 890 W/m^2, the PPVM module has delivered an efficiency of 100%. The efficiency of the PPVM ranges from 95.58% to 100%. For irradiation levels of 580 to 940 W/m^2, the MPVM has performed well, with an efficiency of 90.00%. The efficiency of the MPVM varies between 87.89% to 90.40%. For irradiation between 470 and 940 W/m^2, the LPVM has achieved efficiencies of 97.77% to 99.94%. For irradiation below 470 W/m2, the LPVM has achieved 100% efficiency. The efficiency of the LPVM varies between 96.82% to 100%.

The efficiency of LPVM decreases with increasing solar irradiation and operating temperature. The LPVM performs better under low irradiation conditions. For the irradiation of below 150 W/m^2, the BPVM has delivered efficiency in the range of 99% and for the irradiation of above 150 W/m^2, the BPVM has delivered efficiency of above 100% The BPVM has obtained an average efficiency of 100.96% compared to the LPVM, PPVM, and MPVM by 99.98%, 98.43% and 89.35%.

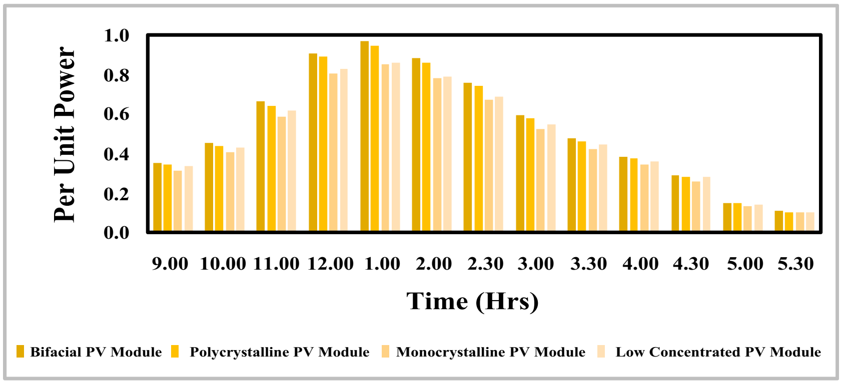

FIGURE 10 | Per unit maximum current of all the PV modules.

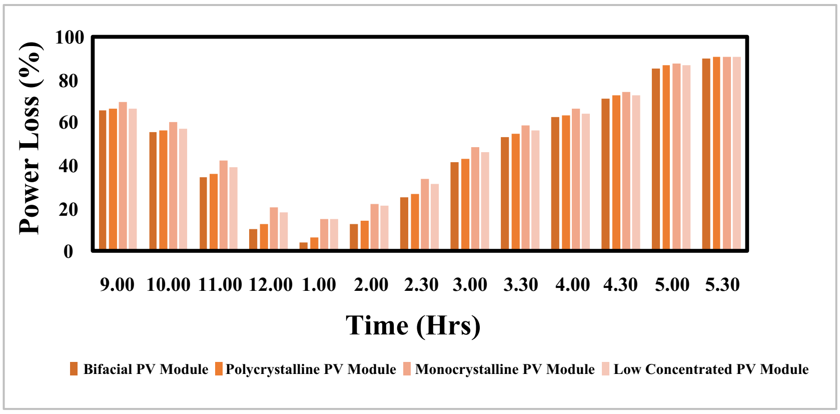

FIGURE 11 | % Power loss of PV module technologies.

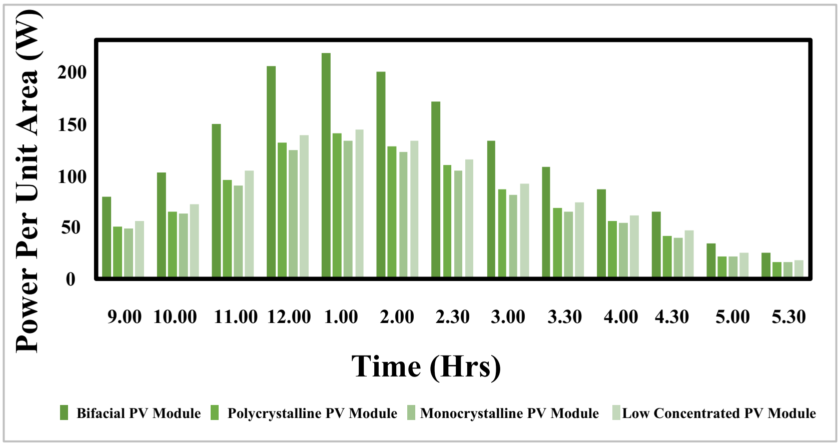

FIGURE 12 | Power per unit area of all PV modules.

3.5 | Power P.U. Area

Figure 12 shows the power P.U. area of all the PV modules considered for the study. At low irradiation of 110 W/m^2, PPVM and MPVM have obtained a P.U. area of 15, and LPVM and BPVM have obtained a P.U. area of 17 and 24, respectively. Here, all the modules have almost the same P.U. area. At high irradiation of 940 W/m^2, the MPVM has obtained the lowest average power P.U. area of 73.46, followed by the PPVM, LPVM, and BPVM at 77, 82.31, and 82.31, respectively. Overall, the BPVM delivers superior P.U. area performance compared to other PV modules.

3.6 | PR

The PR is defined as the ratio of the module's output power under outdoor conditions to its STC. At a low irradiance of 110 W/m^2, the BPVM obtained a PR of 0.985, followed by the PPVM, LPVM, and MPVM at 0.949, 0.941, and 0.878, respectively. Here, the PR of LPVM and MPVM are almost similar. From the results, it is evident that the PR increases with increasing solar irradiation. At the maximum irradiation of 940 W/m^2, the BPVM obtained a PR of 0.102, followed by the PPVM, LPVM, and MPVM with PRs of 0.1000, 0.907, and 0.903, respectively.

From the experimental results, the PR of PPVM operating under low and high irradiation conditions has improved to about 5.08%, followed by the BPVM and MPVM at 3.46% and 2.49%, respectively. The PR ratio of LPVM has decreased by 3.46%. Overall, the BPVM has obtained better PR, followed by the PPVM, MPVM, and LPVM. Figure 13 illustrates that overall, the BPVM has obtained an average PR of about 1.0058, followed by the PPVM, LPVM, and MPVM by 0.978, 0.9368, and 0.8931. The BPVM has shown better performance due to power generation on both sides. Additionally, the white reflecting surface under the module increases the PR by more than 1 due to light reflection from the ground. The N-type PERT BPPV, as per the specification, has the P_{max} of 450 W at 25% ground reflectivity with a bifaciality factor 82%.

3.7 | Comparison of PV Modules

The operating temperature of the PV module increases with increasing solar irradiation. The MPVM has the lowermost operating temperature of 44.62°C followed by the PPVM, BPVM and LPVM by 44.78°C, 46.97°C and 49.84°C. BPVM performance depends on its bifacial gain. Even though the BPVM operates at a higher temperature than the PPVM and MPVM, it yielded better results because of its bifacial gain. The average temperatures of PPVM and MPVM are almost identical. However, PPVM has performed better than MPVM due to its lower PL. Meanwhile, the MPVM operates at a lower temperature than other modules; its P.U. power is lower due to its high PL.

The performance of LPVM is lower due to its high operating temperature; it is suitable for cold climates. Figure 14 shows the average module efficiency of the PV module obtained at the STC. The BPVM has obtained an average module efficiency of 22.72% (at STC = 22.5). The increase in module efficiency is due to the reflector material coating beneath the module. The PPVM operated near its rated module efficiency of 14.47% (at STC = 14.7), followed by the LPVM at 5.73% (at STC = 16.8) and MPVM at 13.87% (at STC = 15.52) (Table 6).

In comparison to the existing research reported in Table 1, the proposed study has compared the performance of the PPVM, MPVM, LPVM, and BPVM. In the study area, the performance of PPVM, MPVM, LPVM, and BPVM was not examined previously. Further, the performance of the LPVM is not explored much. The study results reveal that the performance of BPVM has outperformed with an average module efficiency of 22.72% compared to PPVM (14.47%), MPVM (13.87%), and LPVM (15.73%).

4 | Conclusion

The performance of a PV technology varies with geographical location. It is crucial to determine the appropriate PV technology for a given location. Therefore, this study has analyzed the performance of various PV modules, including PPVM, MPVM, LPVM, and BPVM. The effects of irradiation and temperature on these modules were analyzed in terms of P.U. power, P.U. area, module efficiency, PL, and PR. The study evidenced that the output power increases linearly with incident irradiation and temperature. The module's operating temperature increases with incident irradiance. However, the reduction in output power depends on the module's temperature coefficient. From the results, it is evident that the BPVM can extract power from direct, diffuse, and reflected solar irradiation, and hence it is suitable at high albedo and high latitudes.

The PPVM operates at its rated module efficiency and is less affected by irradiation and temperature changes. The LPVM has operated at a lower module efficiency due to the high operating temperature; hence, it is more suitable for cold climatic conditions. Even though the MPVM operates at almost the same temperature as the PPVM, its performance is low due to its high PL. Overall, the BPVM has delivered higher output power and is less affected by climatic conditions than the MPVM. From this study, it is identified that,

- The power generation P.U. area of PPVM is higher at 139 W/m^2 than that of MPVM.
- The PPVM has a higher PR of 0.978 compared to MPVM and LPVM.
- The average efficiency of PPVM is 14.47%, which operates at a lower temperature than MPVM and LPVM.
- The MPVM has the lowest average temperature of 44.62°C among all modules.
- At low irradiation of 110 W/m^2, the PL produced by all the modules is similar.

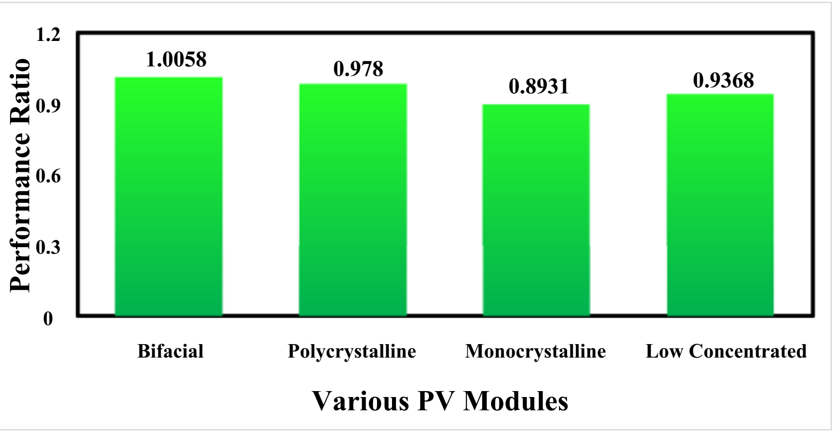

FIGURE 13 | Average performance ratio of all the PV modules.

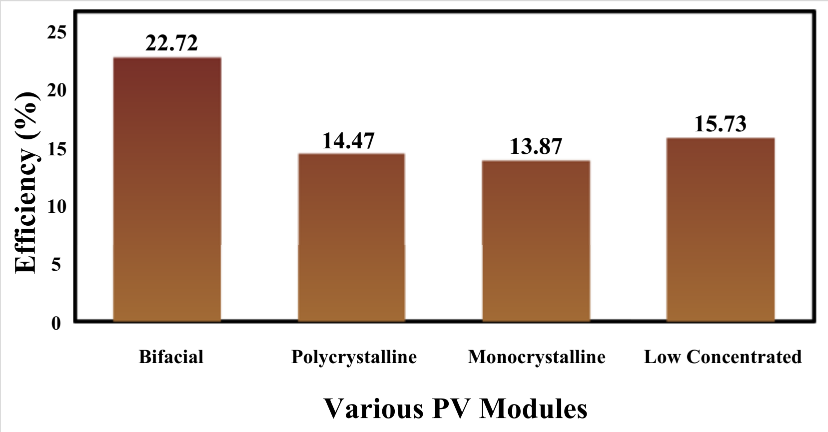

FIGURE 14 | Average module efficiency of PV module technologies.

TABLE 6 | Experimental results for BPVM.

Time	Irradiation (W/m^2)	Temperature (°C)	V_m (V)	I_m (A)	P_m (W)	P.U. V_{max}	P.U. I_{max}	P.U. P_{max}	P.U. area P_m	% PL	% η	PR
9.00	350	39.3	37.5	3.7	138	0.979	0.358	0.350	79	65	22.56	0.9982
10.00	450	43.2	37.6	4.7	178	0.982	0.460	0.451	102	55	22.62	1.0014
11.00	650	49.7	38.0	6.8	260	0.992	0.664	0.658	149	34	22.86	1.0127
12.00	890	52.5	38.1	9.4	357	0.995	0.910	0.904	204	10	22.92	1.0155
1.00	940	58.6	38.3	9.9	379	1.000	0.961	0.960	217	4	23.04	1.0207
2.00	860	56.3	38.2	9.1	346	0.997	0.879	0.876	198	12	22.98	1.0185
2.30	740	53.7	38.1	7.8	297	0.995	0.756	0.751	170	25	22.92	1.0161
3.00	580	51.4	38.0	6.1	232	0.992	0.593	0.587	133	41	22.86	1.0127
3.30	470	48.7	37.7	4.9	187	0.984	0.480	0.472	107	53	22.68	1.0073
4.00	380	42.6	37.6	4.0	150	0.982	0.388	0.381	86	62	22.62	0.9993
4.30	290	39.7	37.5	3.1	114	0.979	0.296	0.290	65	71	22.56	0.9952
5.00	150	37.8	37.3	1.6	59	0.974	0.153	0.149	34	85	22.44	0.9958
5.30	110	37.1	37.0	1.2	43	0.966	0.112	0.108	24	89	22.26	0.9896

- Under high irradiation conditions, the MPVM has obtained higher PL.
- The MPVM operates at a lower temperature than other modules because of its higher PL. The average PR of MPVM is 0.8931.
- The MPVM has the lowest power P.U. area (for 1 m^2) of 132 W/m^2 among all other modules.
- The LPVM operates at a higher temperature and produces higher PL.
- The average efficiency of LPVM is 15.73%, and its power P.U. area is 143 W/m^2.
- The LPVM delivers superior performance at low irradiation conditions.
- The LPVM performs better compared to the MPVM.
- The BPVM has the highest efficiency of 22.72% among all other modules.
- The average PR of the BPVM is highest with the value 1.0.
- The power generation P.U. area is high for BPVM, with 217 W for 940 W/m^2.
- BPVM can generate power from the direct, diffuse, and reflected components of solar irradiation.

In this study, the PPVM, MPVM, LPVM and BPVM are examined under clear sky with lesser occurrence of partial shading. The future scope is to examine the performance of PPVM, MPVM, LPVM, and BPVM under partial shading conditions.

Nomenclature

a-Si	amorphous silicon
BPVM	bifacial PV module
CdTe	cadmium telluride
CIGS	copper indium gallium selenide

CIS	copper indium diselenide
CPV	concentrated PV
c-Si	crystalline silicon
GaAs	gallium arsenide
HCPV	high-concentration PV
HIT	heterojunction with intrinsic thin layer
I_{max}	current at maximum power
I_{sc}	short-circuit current
LPVM	low concentrated PV module
MPVM	monocrystalline PV module
PL	power loss
P_{max}	maximum power
PPVM	polycrystalline PV module
PR	performance ratio
PV	photovoltaic
P.U.	per unit
STC	standard test condition
TPVM	thin-film PV modules
V_{max}	voltage at maximum power
V_{oc}	open-circuit voltage

Author Contributions

Meenatchi Sundaram Palanisamy: conceptualization, formal analysis, investigation, methodology, validation, writing – original draft. **Prince Winston David:** conceptualization, data curation, investigation, methodology, project administration, supervision, visualization, writing – review and editing. **Palpandian Murugesan:** data curation, formal analysis, investigation, methodology, resources, software, writing – review and editing. **Praveen Kumar Balachandran:** conceptualization, formal analysis, funding acquisition, project administration, resources, software, supervision, visualization, writing – review and editing. **Pravin Murugesan:** conceptualization, formal analysis, investigation, methodology, validation, writing – review and editing. **Muhammad Ammirrul Atiqi Mohd Zainuri:** conceptualization, formal analysis, investigation, resources, software, supervision, visualization, writing – review and editing.

Funding

The authors received no specific funding for this work.

Ethics Statement

The paper is not currently being considered for publication elsewhere.

Consent

The authors have nothing to report.

Conflicts of Interest

The authors declare no conflicts of interest.

Data Availability Statement

Data sharing is not applicable to this article, as no datasets were generated or analyzed during the current study.

References

1. I. Andric, A. Kamal, and S. G. Al-Ghamdi, "Efficiency of Green Roofs and Green Walls as Climate Change Mitigation Measures in Extremely Hot and Dry Climate: Case Study of Qatar," *Energy Reports* 6 (2020): 2476–2489.

2. P. Mints, SPV Market Research Update (2018).

3. S. W. Glunz, R. Preu, and D. Biro, *Crystalline Silicon Solar Cells: State-of-the-Art and Future Developments* (Vol. 1) (Elsevier Ltd., 2012).

4. M. Memiche, C. Bouzian, A. Benzahia, and A. Moussi, "Effects of Dust, Soiling, Aging, and Weather Conditions on Photovoltaic System Performances in a Saharan Environment," *Global Energy Interconnection* 3, no. 1 (2020): 60–67.

5. Photovoltaic (PV) Module Performance Testing and Energy Rating—Part 1: Irradiance and Temperature Performance Measurements and Power Rating, accessed on October 01, 2022, https://webstore.iec.ch/preview/info_iec61853-1%7bed1.0%7db.pdf.

6. T. Pavlović, D. Milosavljević, I. Radonjić, L. Pantić, and A. Radivojević, "Application of Solar Cells Made of Different Materials in 1 MW PV Solar Plants in Banja Luka," *Contemporary Materials* 2 (2011): 155–163.

7. M. K. da Silva, M. S. Gul, and H. Chaudhry, "Review on the Sources of Power Loss in Monofacial and Bifacial Photovoltaic Technologies," *Energies* 14 (2021): 7935.

8. B. Parida, S. Iniyan, and R. Goic, "A Review of Solar Photovoltaic Technologies," *Renewable and Sustainable Energy Reviews* 15, no. 3 (2011): 1625–1636.

9. G. Makrides, B. Zinsser, A. Phinikarides, M. Schubert, and G. E. Georghiou, "Temperature and Thermal Annealing Effects on Different Photovoltaic Technologies," *Renewable Energy* 43 (2012): 407–417.

10. C. Cañete, J. Carretero, and M. Sidrach-De-Cardona, "Energy Performance of Different Photovoltaic Module Technologies Under Outdoor Conditions," *Energy* 65 (2014): 295–302.

11. A. Ndiaye, C. M. F. Kébé, A. Charki, P. A. Ndiaye, V. Sambou, and A. Kobi, "Degradation Evaluation of Crystalline-Silicon Photovoltaic Modules After a Few Operation Years in a Tropical Environment," *Solar Energy* 103 (2014): 70–77.

12. B. Sopori, P. Basnyat, S. Shet, V. Mehta, J. Binns, and J. Appel, "Understanding Light-Induced Degradation of c-Si Solar Cells," Proceedings of the 38th IEEE Photovoltaic Specialists Conference (PVSC), Austin, TX, USA, June 3–8, 2012.

13. D. Dirnberger, G. Blackburn, B. Müller, and C. Reise, "On the Impact of Solar Spectral Irradiance on the Yield of Different PV Technologies," *Solar Energy Materials and Solar Cells* 132 (2015): 431–442.

14. N. Martin and J. M. Ruiz, "Calculation of the PV Modules Angular Losses Under Field Conditions by Means of an Analytical Model," *Solar Energy Materials and Solar Cells* 70 (2001): 25–38.

15. S. Gorjian and A. Shukla, *Photovoltaic Solar Energy Conversion: Technologies, Applications, and Environmental Impacts* (2020).

16. N. Romeo, A. Bosio, and A. Romeo, "An Innovative Process Suitable to Produce High-Efficiency CdTe/CdS Thin-Film Modules," *Solar Energy Materials and Solar Cells* 94, no. 1 (2010): 2–7.

17. M. A. Green, E. D. Dunlop, D. H. Levi, J. Hohl-Ebinger, M. Yoshita, and A. W. Y. Ho-Baillie, "Solar Cell Efficiency Tables (Version 54)," *Progress in Photovoltaics: Research and Applications* 27, no. 7 (2019): 565–575.

18. M. Powalla, S. Paetel, E. Ahlswede, R. Wuerz, C. D. Wessendorf, and T. MagorianFriedlmeier, "Thin-Film Solar Cells Exceeding 22% Solar Cell Efficiency: An Overview on CdTe-, Cu (In,Ga)Se 2-, and Perovskite-Based Materials," *Applied Physics Reviews* 5, no. 4 (2018): 041602.

19. W. Metaferia, K. L. Schulte, J. Simon, S. Johnston, and A. J. Ptak, "Gallium Arsenide Solar Cells Grown at Rates Exceeding 300 $\mu m\ h^{-1}$ by Hydride Vapor Phase Epitaxy," *Nature Communications* 10, no. 1 (2019): 3361.

20. A. Woyte, M. Richter, D. Moser, S. Mau, N. Reich, and U. Jahn, *Analytical Monitoring of Grid-Connected Photovoltaic Systems—Good Practices for Monitoring and Performance Analysis* (International Energy Agency (IEA), 2014), 90.

21. R. Gottschalg, T. R. Betts, A. Eeles, S. R. Williams, and J. Zhu, "Influences on the Energy Delivery of Thin Film Photovoltaic Modules," *Solar Energy Materials and Solar Cells* 119 (2013): 169–180.

22. B. Zinsser, G. Makrides, W. Schmitt, G. Georghiou, and J. Werner, "Annual Energy Yield of 13 Photovoltaic Technologies in Germany and in Cyprus," Proceedings of the 22nd European Photovoltaic Solar Energy Conference, Milano, Italy, September 3–7, 2007.

23. R. Ruther, J. Del Cueto, G. Tamizh-Mani, and B. Roedern, "Performance Test of Amorphous Silicon Modules in Different Climates-Year Four: Progress in Understanding Exposure History Stabilization Effects," Proceedings of the 33rd IEEE Photovoltaic Specialists Conference, San Diego, CA, USA, May 11–16, 2008, 1–5.

24. R. Søndenå, Boron-Oxygen-Related Degradation in Multicrystalline Silicon Wafers, www.pv-tech.org.

25. Comparative Study of ILB-ENSOL Modules at Difference Irradiation and Temperature Range, www.ilbhelios.com.

26. S. Krauter, P. Grunow, and S. Lehmann, "The Real Challenges for Photovoltaic Modules," Proceedings of the 25th Anniversary of PASAN, Neuchatel, Switzerland, June 12, 2009.

27. H. Mohring, "Optimized Procedures for Characterization of Module Energy Field," Proceedings of the Integrated Project Performance Final Forum, European Commission, Malaga, Spain, December 11, 2009.

28. A. W. Bett, B. Burger, F. Dimroth, G. Siefer, and H. Lerchenmuller, "High-Concentration PV Using III-V Solar Cells," *Conference Record of the 2006 IEEE 4th World Conference on Photovoltaic Energy Conversion, WCPEC-4* 1 (2007): 615–620.

29. M. Burhan, C. K. J. Ernest, and N. K. Choon, "Electrical Rating of Concentrated Photovoltaic (CPV) Systems: Long-Term Performance Analysis and Comparison to Conventional PV Systems," *International Journal of Technology* 7, no. 2 (2016): 189–196.

30. P. Pérez-Higueras, E. Muñoz, G. Almonacid, and P. G. Vidal, "High Concentrator Photovoltaics Efficiencies: Present Status and Forecast," *Renewable and Sustainable Energy Reviews* 15, no. 4 (2011): 1810–1815.

31. U. A. Yusufoglu, T. M. Pletzer, L. J. Koduvelikulathu, C. Comparotto, R. Kopecek, and H. Kurz, "Analysis of the Annual Performance of Bifacial Modules and Optimization Methods," *IEEE Journal of Photovoltaics* 5 (2015): 320–328.

32. L. Wang, F. Liu, S. Yu, P. Quan, and Z. Zhang, "The Study on Micromismatch Losses of the Bifacial PV Modules due to the Irradiance Nonuniformity on Its Backside Surface," *IEEE Journal of Photovoltaics* 10 (2019): 135–143.

33. G. J. M. Janssen, B. B. Van Aken, A. J. Carr, and A. A. Mewe, "Outdoor Performance of Bifacial Modules by Measurements and Modelling," *Energy Procedia* 77 (2015): 364–373.

34. U. A. Yusufoglu, T. M. Pletzer, L. J. Koduvelikulathu, C. Comparotto, R. Kopecek, and H. Kurz, "Analysis of the Annual Performance of Bifacial Modules and Optimization Methods," *IEEE Journal of Photovoltaics* 5, no. 1 (January 2015): 320–328.

35. S. A. Peláez, "Bifacial Solar Panels System Design, Modeling, and Performance" (Ph.D. thesis, University of Arizona, 2019).

36. L. Burnham, D. Riley, B. Walker, and J. M. Pearce, "Performance of Bifacial Photovoltaic Modules on a Dual-Axis Tracker in a High-Latitude, High-Albedo Environment," Proceedings of the IEEE Photovoltaic Specialists Conference, Chicago, IL, USA, June 16–21 (2019), 1320–1327.

37. A. Asgharzadeh, B. Marion, C. Deline, C. Hansen, J. S. Stein, and F. Toor, "A Sensitivity Study of the Impact of Installation Parameters and System Configuration on the Performance of Bifacial PV Arrays," *IEEE Journal of Photovoltaics* 8, no. 3 (2018): 798–805.

38. C. Hansen, D. Riley, C. Deline, F. Toor, and J. Stein, *A Detailed Performance Model for Bifacial PV Modules (No. SAND2017-11013C)* (Sandia National Lab (SNL-NM), 2017).

39. K. Akhmad, A. Kitamura, F. Yamamoto, H. Okamoto, H. Takakura, and Y. Hamakawa, "Outdoor Performance of Amorphous Silicon and Polycrystalline Silicon PV Modules," *Solar Energy Materials & Solar Cells* 46, no. 3 (1997): 209–218.

40. M. A. MosalamShaltout, A. A. El Hadad, M. A. Fadly, A. F. Hassan, and A. M. Mahrous, "Determination of Suitable Types of Solar Cells for Optimal Outdoor Performance in Desert Climate," *Renewable Energy* 19, no. 1–2 (2000): 71–74.

41. K. Nishioka, T. Hatayama, Y. Uraoka, T. Fuyuki, R. Hagihara, and M. Watanabe, "Fieldtest Analysis of PV System Output Characteristics Focusing on Module Temperature," *Solar Energy Materials & Solar Cells* 75, no. 3 (2003): 665e71.

42. A. J. Carr and T. L. Pryor, "A Comparison of the Performance of Different PV Module Types in Temperate Climates," *Solar Energy* 76, no. 1–3 (2004): 285–294.

43. T. Minemoto, M. Toda, S. Nagae, et al., "Effect of Spectral Irradiance Distribution on the Outdoor Performance of Amorphous Si//Thin-Film Crystalline Si Stacked Photovoltaic Modules," *Solar Energy Materials & Solar Cells* 91, no. 2–3 (January 2007): 120–122.

44. N. Amin, C. W. Lung, and K. Sopian, "A Practical Field Study of Various Solar Cells on Their Performance in Malaysia," *Renewable Energy* 34, no. 34 (2009): 1939–1946.

45. O.-M. Midtgard, T. O. Sætre, G. Yordanov, A. G. Imenes, and C. L. Nge, "A Qualitative Examination of Performance and Energy Yield of Photovoltaic Modules in Southern Norway," *Renewable Energy* 35, no. 6 (2010): 1266–1274.

46. E. Maluta and V. Sankaran, "Outdoor Testing of Amorphous and Crystalline Silicon Solar Panels at Thohoyandou," *Journal of Energy in Southern Africa* 22, no. 3 (2011): 16–22.

47. V. Sharma, A. Kumar, O. S. Sastry, and S. S. Chandel, "Performance Assessment of Different Solar Photovoltaic Technologies Under Similar Outdoor Conditions," *Energy* 58 (2013a): 511–518.

48. N. Aste, C. Del Pero, and F. Leonforte, "PV Technologies Performance Comparison in Temperate Climates," *Solar Energy* 109 (2014): 1–10.

49. A. Al-Otaibi, A. Al-Qattan, F. Fairouz, and A. Al-Mulla, "Performance Evaluation of Photovoltaic Systems on Kuwaiti Schools' Rooftop," *Energy Conversion and Management* 95 (2015): 110–119.

50. A. K. Tossa, Y. M. Soro, L. Thiaw, et al., "Energy Performance of Different Silicon Photovoltaic Technologies Under Hot and Harsh Climate," *Energy* 103 (2016): 261–270.

51. L. R. do Nascimento, M. Braga, R. A. Campos, H. F. Naspolini, and R. Rüther, "Performance Assessment of Solar Photovoltaic Technologies Under Different Climatic Conditions in Brazil," *Renewable Energy* 146 (2020): 1070–1082.

52. R. V. Parupudi, H. Singh, and M. Kolokotroni, "Low Concentrating Photovoltaics (LCPV) for Buildings and Their Performance Analyses," *Applied Energy* 279 (2020): 115839.

53. T. Hariharasudhan, D. Prince Winston, M. Palpandian, and M. Pravin, "A Comparative Analysis of Polycrystalline and Bifacial Photovoltaic Module Under Various Partial Shading Condition," *Energy Conversion and Management* 270 (2022): 116223.

54. H. M. A. Muhammad Anser Bashir, M. A. Shahid Khalil, and A. M. Siddiqui, "Comparison of Performance Measurements of Photovoltaic Modules During Winter Months in Taxila, Pakistan," *International Journal of Photoenergy* 2014 (2014): 898414.